Appendix to final report

Figures, diagrams, contact details, and project logo

Project Name	**InAIPS – Innovative aircraft ice protection system – sensing and modelling**
Project number	326006
Participants	TWT GmbH Science & Innovation (TWT, Coordinator), University of Ioannina (UOI), National and Kapodestrian University of Athens (UOA), GKN Aerospace Services Ltd (GKN)
Deliverable written by	Christine Radermacher (TWT)
Date	29.04.2015

Table of contents

1. Main S & T results/foregrounds

The main objective of the project is a system model for ice detection on laminar flow wings and their impact on the aerodynamic characteristics of the aircraft. The approach as well as the main results and achievements towards this goal are described in the following:

1.1 General idea of the system model

Current ice detectors are usually located remote from the critical aerodynamic surfaces (such as the wing) and as such can lead to the ice protection system being triggered in an inefficient manner by activating it long before ice actually starts forming on the wing. The detection of ice on the wing surface, especially for new laminar wing concepts that are particularly sensitive to the presence of ice, therefore allows a more efficient use of the IPS by only activating it when it is needed. To overcome the remote location of current ice-detection systems, the approach of the Clean Sky project InAIPS is based on aero-conformal optical ice detection sensors which are integrated directly into the leading edge of the wing at the relevant positions. The sensor signals are then translated to ice thickness and ice type using an algorithm based on an Ensemble-Kalman Filter technique. The sensing technology and the dedicated algorithm were first developed in the EU FP7 project ON-WINGS. The InAIPS objective goes beyond the ON-WINGS approach by using several sensors and integrating them in a system model which combines the information on the ice accretion with aerodynamic simulations. The final model can be used to assess the impact of the icing of a wing section on the general aerodynamic asymmetry of the aircraft for various flight conditions.

1.2 Ice detection sensor technology

In the InAIPS project two different types of ice detection sensors were developed. The first type relies on detecting the backscatter and reflected of light from the ice volume using a fibre array geometry. This sensor type was mounted in two positions on the leading edge of the laminar flow wing, one on the stagnation line and the other one on upper surface of the leading. The second type of sensor was a surface-mounted quasi-distributed ice sensor relying on optical losses induced by the presence of ice on the surface of the wing. Figure 1 shows the sensor setup on the physical aerofoil model.

Figure 1: The sensor setup(left) and the test bed aerofoil mounted in the ice tunnel (right).

The array fibre sensor consists of a central source fibre and three signal fibres on either side and is a further development of the ice sensor originally developed in the ACIDS and ON-WINGS projects. The further development of this technology undertaken in the InAIPS project was the optimization of a similar sensor architecture for the specific needs of this project, namely the detection of very thin ice, which is particularly disruptive to the laminar flow of the wing. The general principle of this sensor technology is displayed in Figure 2.

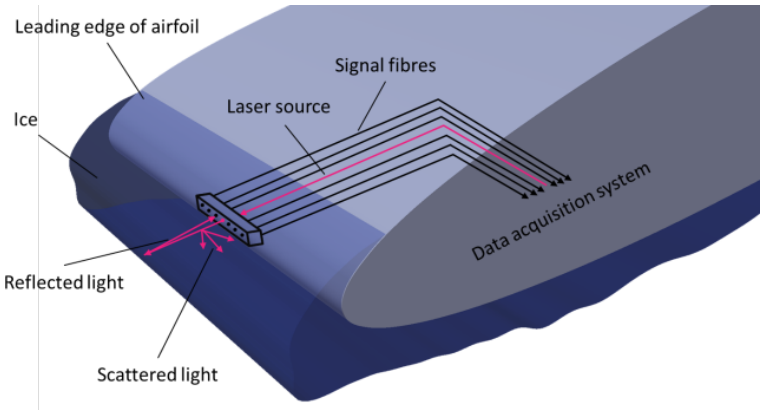

Figure 2: General principle of the optical sensor for ice detection.

In addition to the array fibre optical sensors, a distributed ice/no ice sensor was installed to indicate the existence of ice behind the erosion shield. The sensor, in this flash format, is a new development and was tested in InAIPS for the first time. It consists of four sensor units, which were integrated in different glass fibres and a light source fibre. The sensor assembly was mounted on the upper surface of the wing inside a groove specially designed to house the sensor.

The distributed ice sensor was an experimental sensor and as such there is still a need for further development. It performed well in the lab experiments, but when located on the wing, it was not possible to position it in a high ice accreting area, without affecting the airflow and consequently it did not reveal its full potential. In fact some ice was accreting and then flaking off, giving a very erratic signal response which was thus inconclusive.

1.3 Data acquisition system

The signal data measured by the sensors is collected by a data acquisition system constituted of an optical interface with 24 photodiodes. The signal transfer from the sensors is realized through ST/PC fibre optical connectors. The data are transferred to a host PC and handed to the post-processing software via a USB port.

1.4 Ice detection algorithm

The signals from the optical fibres in the sensors collected by the acquisition system are processed by an ice detection algorithm, which translates the signals to thicknesses based on an Ensemble Kalman-Filter (EKF) technique. The underlying algorithm was first developed during the FP7 project ON-WINGS. In the InAIPS project, the algorithm was tested in coincidence for both array sensors. The ice thicknesses measured during the icing wind tunnel tests serve as basis for a look-up-table (LUT), to determine the thickness from the measured intensity and evaluate the corresponding outside air temperature. The smoothed sensor signals, of which the LUTs are constituted, are shown in Figure 3.

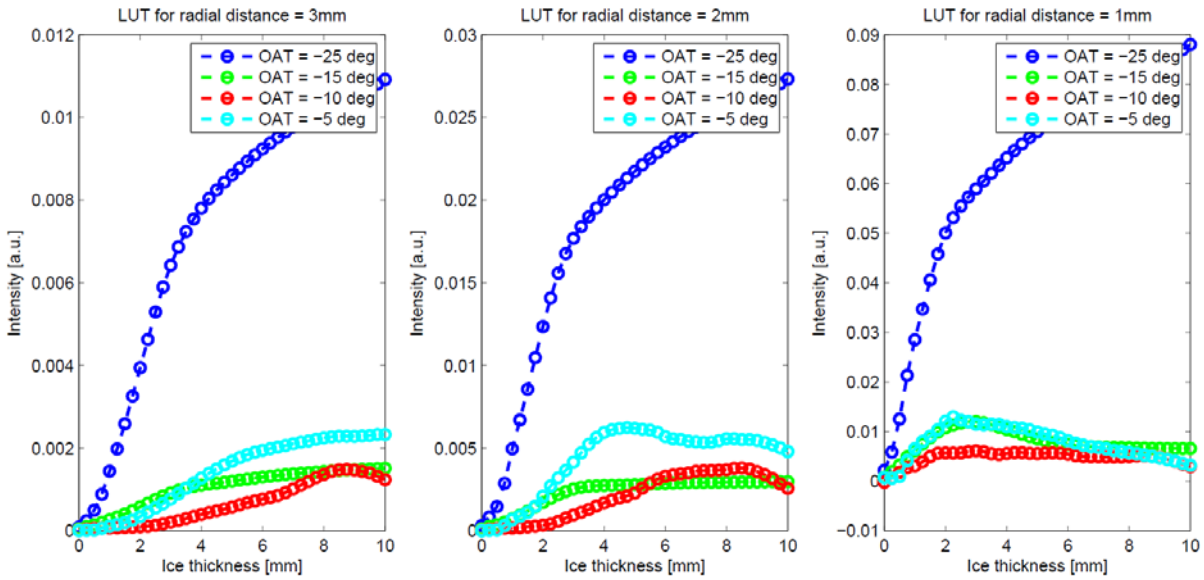

Figure 3: Smoothed and averaged sensor data. a) Data for radial distance of 3 mm (channels 1 & 6). b) Data for radial distance of 2 mm (channels 2 & 5). c) Data for radial distance of 1 mm (channels 3 & 4).

Validation of the methodology showed good performance for the determination of the ice thickness. For the evaluation of the ice type and the corresponding outside air temperature it had some shortcomings at glaze ice conditions, i.e. higher temperatures.

The performance of the methodology is to a large extent constrained by the quality of the LUT, which is compiled from the data acquired during the InAIPS wind tunnel tests. By performing tests for the same conditions repeatedly and covering a range of temperatures and angles of attack, a good set of data could be obtained. Nevertheless, the parameter space is limited. Independency of such LUTs could be reached by using a physical model of the photon intensity to derive ice parameters from the backscattered intensities. The time frame of the InAIPS project did not allow the development and validation of such a model, but these tasks could be subject to possible follow-up activities.

1.5 CFD simulations

The shape of the laminar flow wing was used as input geometry for computational fluid dynamics (CFD) simulations to investigate the lift and drag forces on the aerofoil section. The incompressible, stationary simulations were carried out with a Spalart-Allmaras model that was run with an RANS solver. After first simulations with the ice-free wing geometry, sensitivity tests with generic ice shapes of different size and under different conditions were carried out and analysed. When a first set of measurement data had been obtained during the ice tunnel tests in August 2014, the real ice shapes were digitized and their geometry was meshed. The geometries were used to carry out CFD simulations for the iced wing section under the same conditions as for the ice tunnel measurements. By visual inspection and by analysis of the section lift and drag coefficients, the influence of the icing on the flow characteristics under different angles of attack, temperatures, and ice shapes was investigated.

The simulation results for six different icing situations are shown in Figure 4 and Figure 5.

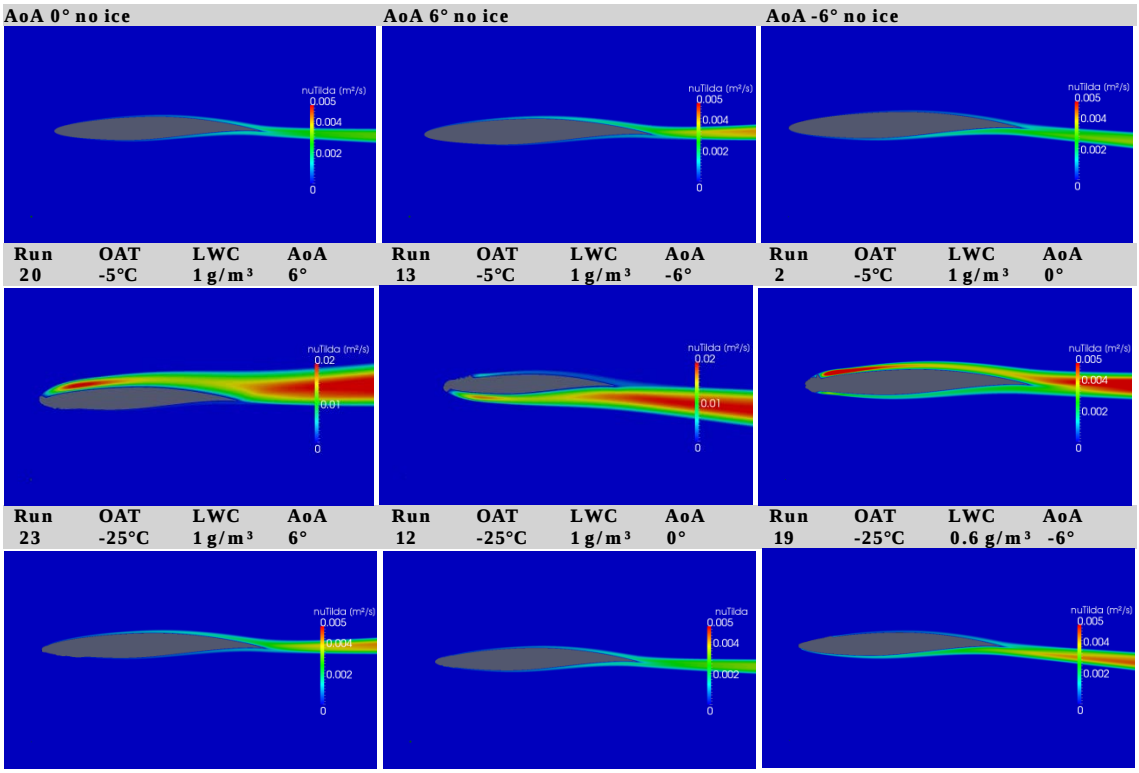

Figure 4: CFD-Results for the distribution of the turbulent kinematic viscosity around the aerofoil for three cases without ice and different angles of attack and for six different icing situations. Note the different scale for Run 20 and 13.

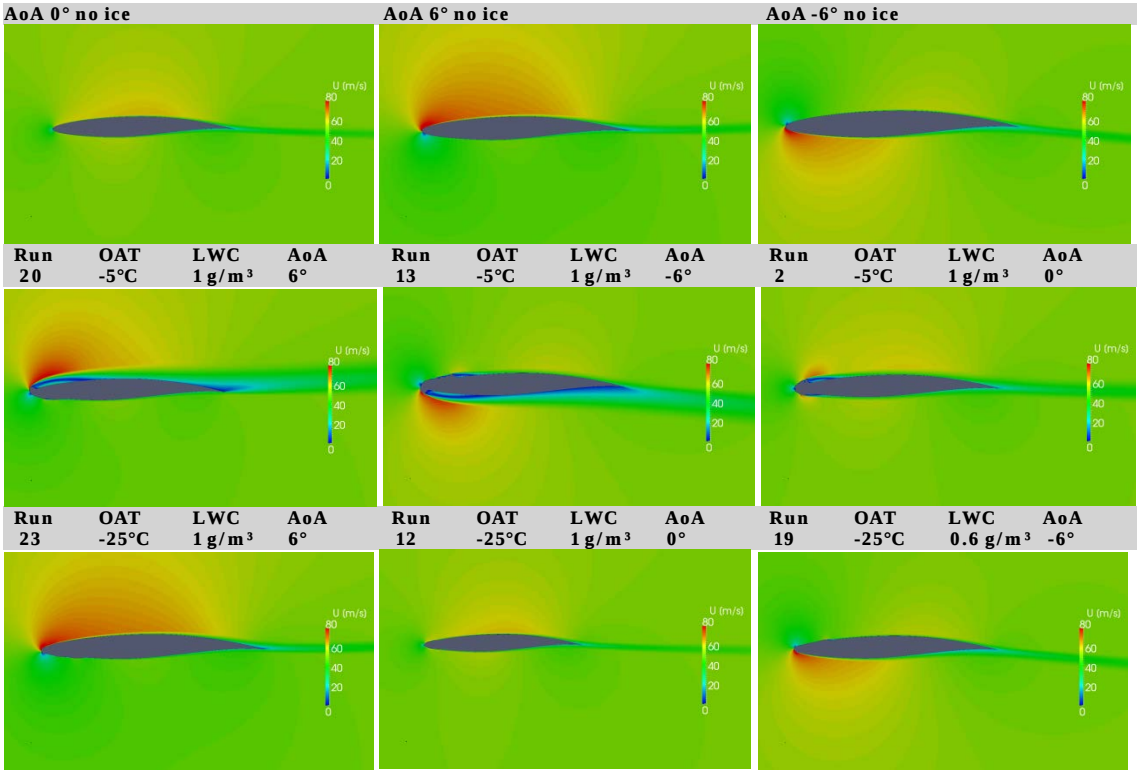

Figure 5: CFD-Results for the distribution of velocity (U [m/s]) around the aerofoil for three cases without ice and different angles of attack and for six different icing situations.

1.6 System model

Based on the developments on the sensor, the ice detection model and the CFD simulation, the system model was constituted from the pieces described before. The structure of the system model is given in Figure 6.

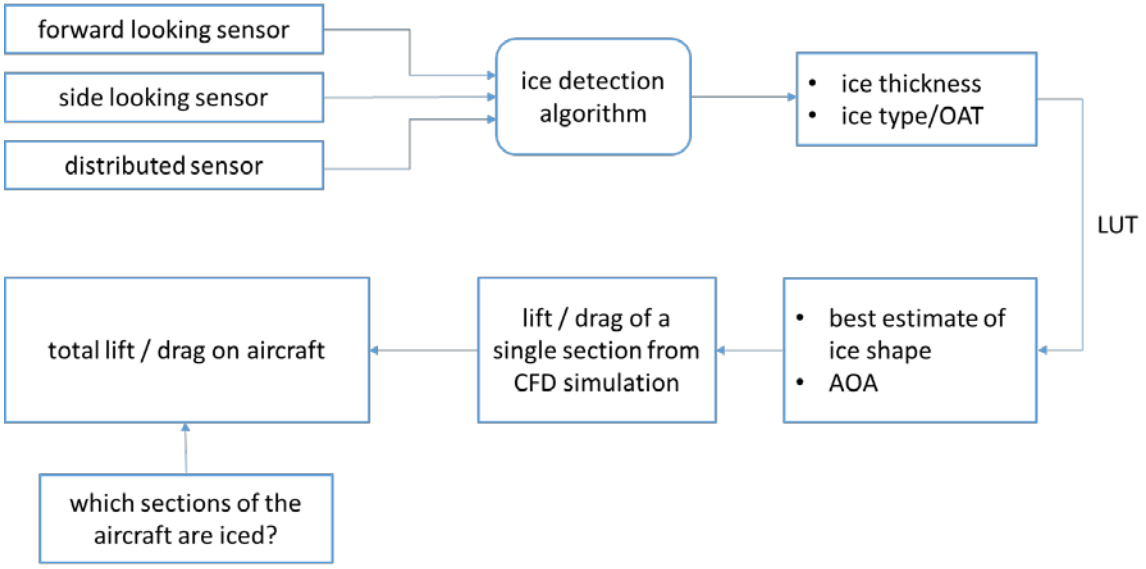

Figure 6: Structure of the InAIPS system model

The functionality of the model can be summarized as follows: The raw data from the optical sensors is fed to the EKF algorithm which translates the intensities to ice thicknesses and evaluates ice type and outside air temperature based on the progress of the intensity signal with ice growth.

From the ice thicknesses detected by both sensors, other parameters can be derived. Factors including the icing conditions and the wing's angle of attack cause ice to accrete unevenly around the wing's leading edge, i.e. for a positive angle of attack, more ice accretes on the lower edge of the wing, and vice versa. Therefore, the thickness ratio (TR) of the forward looking sensor and the upward looking sensor is a good indicator for the angle of attack and gives a best guess for the shape of the ice. This is illustrated in Figure 7. Although there is a clear relationship between the angle of attack and the accreted ice shape for the InAIPS aerofoil profile, this is not necessarily true for all aerofoils.

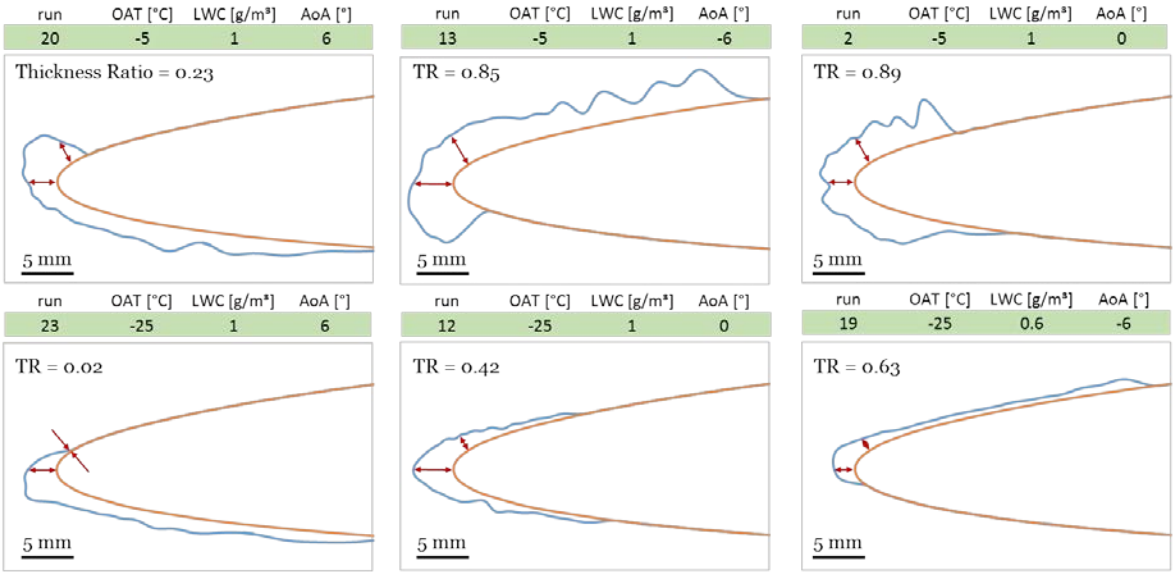

Figure 7: Six characteristic measured ice shapes (blue) and the aerofoil profile (orange). The thickness ratio (TR) between the side looking sensor and the forward looking sensor is given.

Based on the ratio of the thicknesses measured by the setup of the optical sensors, the ice shape is determined and the corresponding CFD simulation determines the lift and drag on the aerofoil.

The final system model should give an estimate of the ice layer's current influence on the aircraft's aerodynamic behaviour. Therefore, a linear shrinking algorithm has been applied to calculate ice profiles of different thickness from the original shapes. These are used to perform ice thickness dependent CFD simulations on characteristic shapes from the icing tunnel tests. The results of these CFD simulations, which are summarized in Table 2, are the lift and drag coefficients of the iced airfoil section for different ice thicknesses.

Table 1: Ice thickness dependent lift and drag coefficients from CFD simulations

icing tunnel parameters	digitized ice shape from August 2014 tests, virtually shrunk	lift coefficient vs ice thickness	drag coefficient vs ice thickness
OAT = -5° AoA = -6°	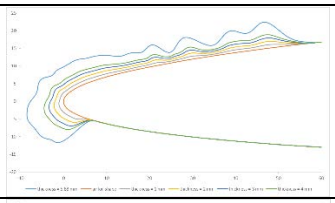	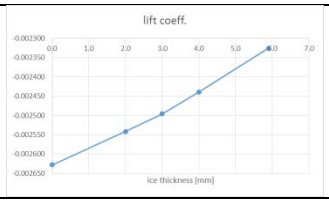	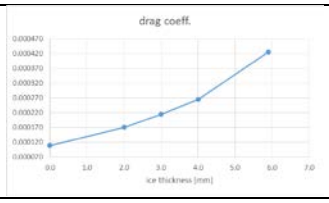
OAT = -5° AoA = 0°	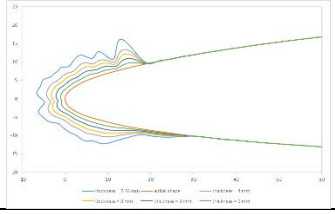	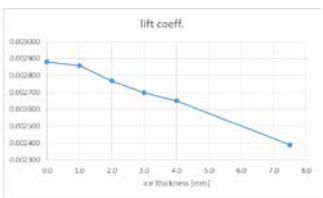	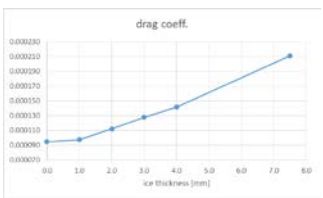
OAT = -5° AoA = +6°	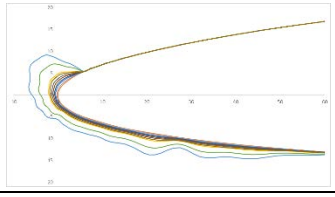	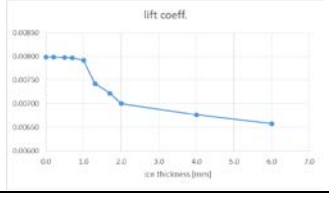	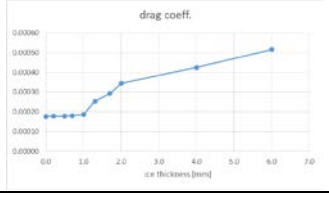

OAT = -25° AoA = 0°	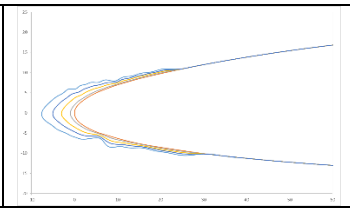	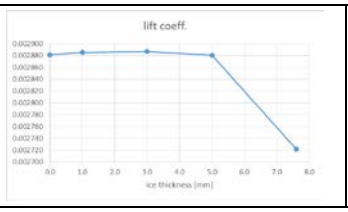	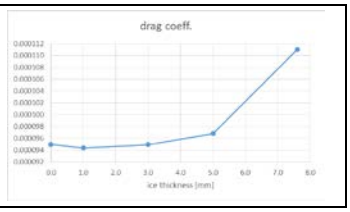

The results have shown strong dependencies of lift and drag on the ice thickness. Even for a thin layer of ice the effect can be immense. In Table 2 the changes in the section lift and drag coefficient for an aerofoil with 2mm ice thickness compared to an ice-free aerofoil are displayed for different flight conditions. The decrease of the lift and increase of the drag is particularly large for climb flight conditions.

Table 2: CFD-simulated changes in lift and drag of the aerofoil profile with 2mm compared to the un-iced profile.

Case	Lift change	Drag change
OAT -5°C/AoA -6°	-5%	42%
OAT -5°C/AoA 0°	-4%	22%
OAT -5°C/AoA 6°	-13%	94%
OAT -25°C/AoA 0°	0%	0%

The model was finally extended to the assessment of the aircraft's wing asymmetry due to icing. Ice accreted on an aircraft's wing can have a strong influence on the aircraft's aerodynamics. A strong asymmetric behavior can even render the aircraft difficult to control. Therefore, based on the information on the ice thickness, one can assess the force asymmetry and therewith the rolling and yawing moments on the aircraft, which is described in the following.

The lift force per unit span is defined as

$$l = \frac{1}{2} c_l \rho v^2 c,$$

where c_l is the lift coefficient, ρ the air density, v the true airspeed and c the chord of the airfoil. Analogously, the drag force per unit span is defined as

$$d = \frac{1}{2} c_d \rho v^2 c,$$

where c_d is the drag coefficient. We obtained c_l and c_d from realistic CFD calculations for different ice shapes and thicknesses (see Table 1). To obtain the total lift L and the total drag D, l and d must be integrated over the extension of the airfoil:

$$L = \int_{-X/2}^{+X/2} l \, dx,$$

$$D = \int_{-X/2}^{+X/2} d \, dx,$$

where X is the full span of the airfoil and dx an infinitesimal length along the span, at position x. L and D can now be compared to ice-free values and the severity of the ice accretion can be estimated. However, these values do not give information on the force asymmetry. For this purpose, the rolling moment M_r and the yawing moment M_y need to be considered:

$$M_r = \int_{-X/2}^{+X/2} l \, x \, dx,$$

$$M_y = \int_{-X/2}^{+X/2} d \, x \, dx,$$

These considerations are used to estimate the discussed quantities in the Matlab/Simulink tool (see next section).

1.7 Graphical User Interface

An existing Matlab/Simulink tool for system model testing has been further advanced for the purposes in InAIPS. A screenshot of the graphical user interface (GUI) is shown in Figure 8. In the upper panels the GUI shows the raw data and the current ice thickness as obtained from the two independent Ensemble Kalman-Filters (Figure 8a to d). The centre left panel of the GUI depicts the best estimate of the current ice shape (Figure 8e). Further, it informs the user about the current estimated AoA and the OAT. In the GUI's central panel information on the current estimate for lift and drag is shown (Figure 8f). The user has the possibility to indicate the iced section on the aircraft and the GUI shows the total calculated lift and drag for the aircraft and also indicates the change with respect to the ice free lift and drag in percent. The system further calculates the resulting rolling and yawing moment. The lower left panel visualises the behaviour of the de-icing heater system. The lower right panel shows the control variables.

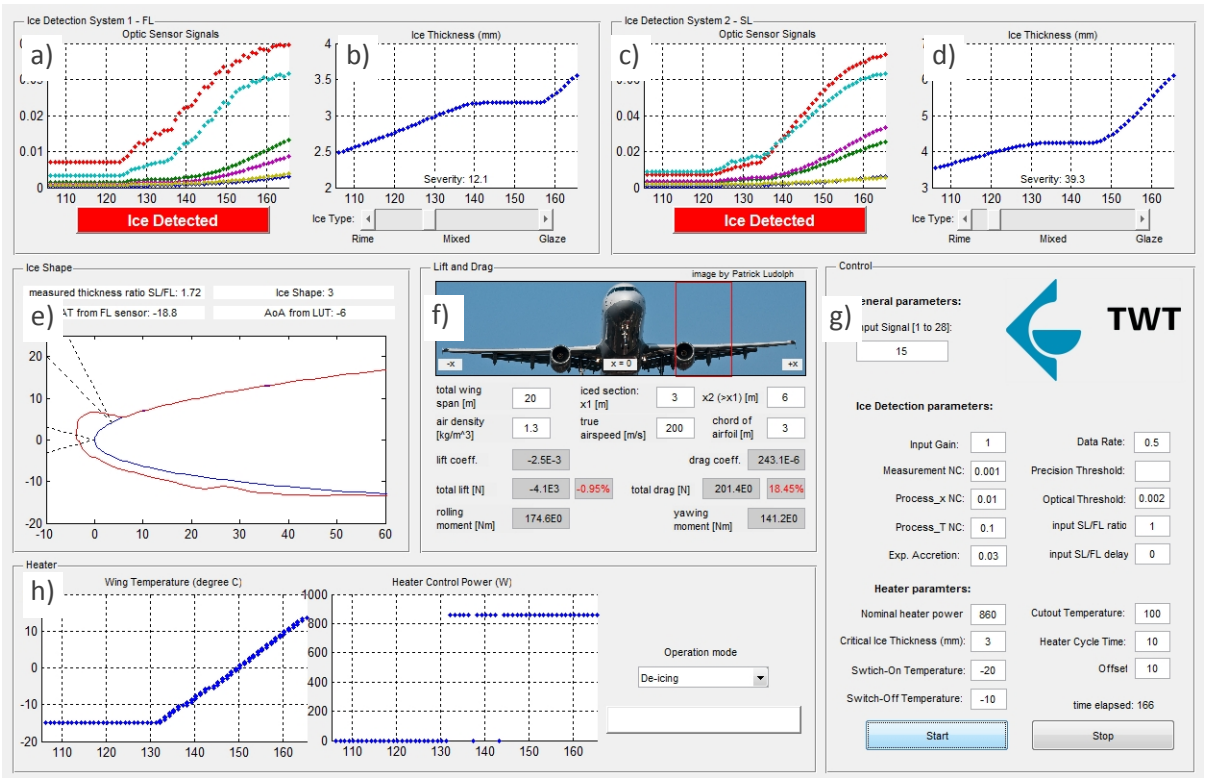

Figure 8: System model graphical user interface (GUI). a), c) Optical sensor signals from forward looking (FL) and side looking (SL) sensor, respectively. b), d) EKF estimated ice thickness for FL and SL sensor, respectively. e) Ice shape estimation and visualisation. f) Lift and drag estimation and calculation of rolling and yawing moments. g) Control parameters. h) Heater system information.

The evaluation of the total lift and drag forces on the wing as well as the rolling and yawing moments allows to assess how critical the icing of a wing section is for the flight characteristics of the laminar flow wing, or, in the context of an Ice Protection System (IPS), how critical the failure of a certain de-icing section would be. The system model is thus a useful tool to investigate the number of

independent de-icing zones needed to ensure flight safety even in the case of partial failure of one or more zones

2. Contact details

The contacts of the consortium members are given in the following table:

Partner	Person	Role	Email
TWT GmbH	Christine Radermacher	Project coordinator	christine.radermacher@twt-gmbh.de
University of Ionannina	Aris Ikiades	Assistant Professor	ikiadis@uoi.gr
University of Athens	Dimitris Syvridis	Professor	dsyvridi@di.uoa.gr
GKN Aerospace	Thomas Richards	Project Engineer	thomas.richards@gknaerospace.com

3. Logo